Colloids and Surfaces A: Physicochemical and Engineering Aspects

Hierarchical Surface Coatings of Polystyrene Nanofibers and Silica Microparticles with Rose Petal Wetting Properties

Michael T.Y. Paul, Byron D. Gates*

Department of Chemistry, Simon Fraser University, 8888 University Drive, Burnaby, B.C. V5A 1S6, Canada

ABSTRACT

Surfaces with rose petal like properties, simultaneously exhibiting a high degree of hydrophobicity and a high adhesion to water, were prepared by spray coating of progressively smaller hydrophilic silica particles along with hydrophobic nanofibers onto surfaces of interest. Various polymer structures were achieved by tuning the spray coating flow rates during deposition of the polymer nanofibers and silica particles. At a reduced flow rate, polystyrene fibers were formed with diameters of less than 100 nm. Water contact angles (WCAs) of coatings prepared from the hierarchical assemblies of silica particles blended with polystyrene nanofibers were greater than 110°. Coatings prepared from the hierarchical assemblies either with or without incorporation of the polymer nanofibers pinned water droplets to their surfaces even after inverting the substrates, similar to the properties of a rose petal. Hierarchical coatings of silica particles without the polystyrene nanofibers also exhibited a high adhesion to water, pinning at least 30% more water on its surfaces. Conversely, hierarchical coatings containing the polystyrene nanofibers exhibited an increased water mobility across their surfaces. Further water retention experiments were performed to determine the ability of the different coatings to efficiently condense water vapor, as well as their efficiency to remove this condensed liquid from their surfaces. Both types of hierarchical coatings exhibited an excellent ability to retain water at a low humidity, while establishing a self-limiting condition for retaining water at a high humidity. These coatings could be prepared on a relatively large-scale and with a relatively low cost on the surfaces of a variety of materials to enhance their water resistance, water retention and/or ability to condense water vapor.

KEYWORDS: rose petal surfaces; hierarchical structures; silica particles; nanofibers; surface modification; water adhesion

INTRODUCTION

One of the more interesting characteristics of microstructured surface textures observed in nature are those of rose petals. The surfaces of rose petals exhibit a strong hydrophobicity, while simultaneously displaying a high adhesion to water droplets even when the surfaces are inverted by 180 degrees. Rose petal surfaces contain distinct features with dimensions that can be classified on at least two different scales *(1-13)*. The hierarchical roughness of these surfaces enables water droplets to penetrate into the void spaces between the larger, microscale structures while limiting further wetting and penetration of water into the surfaces with the inclusion of nanoscale hydrophobic features *(3-9)*. The wetting properties of rose petal surfaces is a delicate balance between the Cassie-Baxter state *(14)* — where a water droplet is supported on surfaces with entrapped air pockets — and the Wenzel state *(15)* — where a water droplet is fully wetting the surfaces.

The wetting properties of microstructured surfaces are of widespread interest for their self-cleaning *(16, 17, 18)*, anti-reflection *(19, 20)*, and fluid drag reduction *(21)* properties. These characteristics of surface coatings can be achieved through chemical modifications *(22, 23)* and/or the addition of microstructures *(6-10, 24, 25)*. Many natural biological materials, such as lotus leaves *(26)*, water strider legs *(27)*, and avian feathers *(28, 29)*, possess specialized water repelling surfaces. Variations in surface micro- and nanostructures can further transform hydrophobic surfaces into adhesive materials that have similar properties and structures as a gecko's foot *(30, 31)*, and a spider's leg *(32)*.

Applications in creating surfaces with an enhanced water resistance, improved capability of collecting water, and/or proficiency in maintaining moisture has inspired many researchers to prepare rose petal like surfaces. Many studies have demonstrated that the opposing water wetting states, namely hydrophobicity and hydrophilicity, of surfaces can be tuned by varying the dimensions of micro- and nanostructures (*2-12*). One method for preparing surfaces with well-defined structures uses reactive ion etching to prepare regular arrays of cylindrical silicon nanopillars *(12)*. By tuning the reaction conditions, silicon protrusions can be created with conical or pyramidal asperities and average heights of ~10 micrometers and can be further tuned to mimic hierarchical structures *(33)*. Structured surfaces prepared

by this semiconductor fabrication process can achieve very high water contact angles (WCAs) of ~150 degrees, and exhibit a high adhesion for water droplets even when the substrate was inverted. Nanoimprint lithography has also been used to prepare surfaces with the desired water wetting and adhesion properties. Some examples include the use of biological templates and nanoimprint lithography with lotus leaves, butterfly wings, and rose petals *(34-37)*. However, each of these techniques are relatively expensive due to the required equipment. To reduce costs, researchers have used relatively inexpensive materials, such as vapor deposited polystyrene nanopillars *(38)*, parylene nanofibrillar structures *(39)*, plasma etched and structured polydimethylsiloxane films *(40)*, hydrothermally deposited antimony oxide films *(41)*, and zinc oxide nanorods *(42)* to mimic rose petal like surfaces. Although these methods are relatively inexpensive, the surface areas coated by each process are still limited by equipment constraints. For example, the size of the chambers for vapor deposition or plasma etching will ultimately limit the maximum dimensions of the coated surfaces. There are still further challenges to apply these methods and materials to modifying larger areas and other surfaces, such as the exteriors of buildings or interior walls, for the purposes of managing water retention and transport.

In this study, we pursue a relatively inexpensive method for preparing rose petal inspired surfaces. A simple and quick method was developed to prepare coatings on a variety of substrates that combined spray coating of silica particles with the simultaneous formation of nanofibers from a polystyrene binder. These spray coating techniques could be extended to prepare coatings that cover relatively large areas. Coatings were prepared in a layer-by-layer fashion with a decreasing size of silica particles with increasing thickness. These hierarchically assembled coatings of silica particles with the inclusion of polymer nanofibers exhibited a large WCA hysteresis that is a distinguishing characteristic of rose petal surfaces. By tuning the conditions for deposition of the silica particles and polymer binder, the surface topographies were further tuned to increase or decrease their hydrophobicity while retaining a relatively high adhesion to water when inverted. Through the development of the techniques outlined in this study, rose petal inspired surfaces for potential use in interior or exterior environments could be

pursued on a relatively large scale as required for a variety of applications in the management of water adhesion and/or transport.

MATERIALS AND METHODS

Preparation of Structured Surfaces. Two types of silica particles, smaller particles (200 mesh particles with measured diameters between 1 and 250 μm) and larger particles (40 mesh particles with measured diameters below 500 μm), were purchased from Mallinckrodt Silica AR® and B. Braun Melsungen AG, respectively. Polystyrene (45,000 M.W.) that was used as a binding agent for these silica particles was purchased from Sigma-Aldrich. These materials were spray coated using an airbrush coater (Crescendo 175®) purchased from Badger Air-Brush Company. All solvents used in this study were purchased from Sigma-Aldrich. The solutions prepared for spray coating contained mixtures of silica particles and polystyrene binder suspended in toluene. These mixtures were deposited by spray coating onto flat glass substrates from a distance of 30 cm while tuning the air flow parameters (with ranges tuned between 2.4 and 12 mL/min) to achieve different surface topographies. Glass microscope slides were chosen as the test substrate for these studies because they are relatively smooth and flat, ensuring consistency in sample preparation and characterization between samples (e.g., WCA measurements). This technique can be extended to directly coat non-porous surfaces (i.e. polymers, or polymer coated panels) or porous surfaces (e.g., concrete, or cellulose based fiber boards) that are first sealed with a thin coating of polymer. The solution of polystyrene binder was prepared by dissolving polystyrene at 30 % (w/v) into toluene.

The silica particles were mixed with the binder solution in a 1:9 ratio (w/w) of silica to binder solution. This mixture was first agitated by repeatedly withdrawing and dispensing the solution (at least 10 times) with a glass Pasteur pipette and subsequently used in the spray coating process. The nozzle of the spray coater was held at a distance of 30 cm from a vertically mounted substrate, and the spray coater pressurized with nitrogen gas (99.995%) at 20 psi. The distance of 30 cm was chosen based on a systematic investigation into the degree of solvent residue in the spray coated films, which influenced

their adhesion to the surfaces and the desired topographies, as well as the uniformity and area of coverage achieved during the spray coating process. To prepare the hierarchical structures, the reservoir of the spray coater was first loaded with a 2 mL solution of the larger silica particles suspended in toluene, which was deposited onto the target substrates at a flow rate of 12 mL/min. This step was followed by spray coating a solution containing the smaller diameter silica particles using identical deposition conditions. An additional drying step of at least 10 min was included between depositing each layer of the coating. To prepare coatings that contained nanoscale fibers of polystyrene, spray coating procedures were used that were akin to those used in preparing the hierarchical structures. This method was modified to include a reduced flow rate of ~2.4 mL/min when preparing each layer during the spray coating process. Coatings were also prepared that contained only a solution of dissolved polystyrene or a suspension of one type of silica particles as control samples for comparison with these two different types of hierarchical structures (i.e. those with and without the inclusion of polystyrene nanofibers).

Characterization of Structured Surfaces. The structured coatings prepared in these studies were characterized using optical microscopy, scanning electron microscopy (SEM), and water contact angle (WCA) measurements. The topographies of and structures within the as-prepared surfaces were examined using a Carl Zeiss Axio Imager M1m optical microscope, or an FEI™ Helios NanoLab DualBeam™ SEM operating with an accelerating voltage of 1 kV and with a potential of 1 kV applied to the sample stage to minimize sample charging. To determine the properties of these surfaces for the adhesion, retention and overall management of water, a series of WCA measurements were performed on images obtained when various aliquots of 18 MΩ-cm deionized water (volumes ranging from 10 to 100 μL) were applied to the structured surfaces. These WCA analyses were obtained for substrates held at a series of pre-defined tilt angles that included 0, 45, and 180 degrees. Images depicting a profile view of the samples during these tests with an increasing volume of water aliquoted onto their structured surfaces were captured with a Canon® PowerShot S110, and their water contact angles determined using Adobe Photoshop CS.

RESULTS AND DISCUSSION

Rose petal inspired surfaces were prepared by creating structured surfaces from the deposition of mixtures of silica particles and a polystyrene binder by scalable spray coating processes. Structures contained within these coatings were analyzed by optical microscopy and SEM. The water management properties of these modified surfaces were assessed through a series of WCA measurements for different water droplet volumes monitored over a range of substrate tilt angles. These studies demonstrate the spray coating parameters necessary to prepare a variety of structured surfaces for controlling the management of water, such as promoting adhesion and controlling the retention and penetration of water on these surfaces.

Surface Topographies

The topographies of the structured surfaces prepared by spray coating were tuned to produce hierarchically assembled coatings of silica particles, as well as hierarchical structures with inclusions of polystyrene nanofibers. The SEM analysis of these samples indicated that the outer-most surfaces of the hierarchically assembled structures deposited by spray coating mixtures of silica and polystyrene at a rate of 12 mL/min contained primarily particles with diameters from 7 to 23 μm (Figure 1a). Decreasing the rate of solvent consumption during spray coating to 2.4 mL/min, the top most layer of the final coating contained predominately silica particles with diameters from 1 to 10 μm (Figure 1b). Furthermore, the later sample contained silica particles entangled within a fibrous network of polystyrene. These nanofibers had diameters between 50 and 150 nm with lengths of several micrometers (Figures 1b and 1c). The discrepancy between the minimum feature sizes within these two types of hierarchically assembled samples was attributed to the influences of changing the rate of solution consumption during spray deposition on the final topography and composition of the coatings. It is possible that the smaller silica particles, with diameters less than 10 μm, were preferentially incorporated into the polystyrene

binder within the less turbulent flow at the lower flow rates (2.4 mL/min). Other possibilities are that the portion of silica particles reaching the samples were separated by size within the spray stream either due to turbulent flow at higher flow rates, or that there was an insufficient momentum at lower flow rates to carry the larger particles over the 30 cm distance of separation between the spray nozzle and the target substrates. Alternatively, coating the substrates at high flow rates could result in an insufficient evaporation of the solvent (toluene) before coating the substrate, where the residual solvent could induce reorganization and clustering of the smaller silica particles during the process of solvent evaporation.

Polystyrene nanofibers were incorporated into the layers of silica particles as a result of the decreased rate of solvent consumption during the spray coating process. This adjustment minimized solvent induced clustering of the smaller silica particles, but also resulted in the near complete evaporation of toluene from the polystyrene binder before it reached the target substrate. The SEM analysis indicated that the polymer nanofibers extend radially from the silica particles achieving maximum lengths of ~25 μm and either self-terminated or terminated by bridging between neighboring silica particles (Figure 1c). The presence of the silica particles aided the formation of the polymer nanofibers. Each silica particle served as an anchor point and structural support for the formation of multiple polystyrene nanofibers during solvent evaporation. Similar fibrous structures of polymer have been previously prepared by electrospinning and electrospraying methods *(43, 44)*. However, the method demonstrated herein produced polymer nanofibers of similar dimensions using a relatively simple setup and readily available, off-the-shelf equipment. Surface coatings prepared from a network of fibrous structures—such as assemblies of nanowires *(45, 44)* and chemically etched silicon dioxide *(12)* and polydimethylsiloxane films *(40)* —can greatly increase the hydrophobicity of a material. These fibrous structures reduce the surface area in contact with a water droplet and retain trapped pockets of air within the interconnecting fibrous network. The water management properties of the coatings prepared from spray coating of silica and polystyrene were further investigated through a series of WCA measurements.

Static WCA Measurements

Static WCA measurements were performed to assess the water management properties of the structured surfaces. Droplets of deionized water (10 μL) were placed in random locations across the test surfaces for the WCA measurements. These measurements were performed while keeping each of the substrates flat (Figure 2). The WCA values were also measured for a series of control samples. These samples were prepared by spray coating separate films of only polystyrene, the smaller silica particles with polystyrene binder, and the larger silica particles with polystyrene binder. The average WCA values for these controls were 43, 87, and 97 degrees, respectively. In contrast, samples prepared from the hierarchical assembly of silica particles had a WCA value of 106 degrees, and samples of hierarchically assembled silica particles with the inclusion of polystyrene nanofibers had a WCA value of 111 degrees. However, due to the high degree of surface roughness and the dielectric properties of these structured coatings, it is challenging to determine the exact interface between the water droplet and the substrate (Figure 2). Therefore, the WCA measurements are likely underestimated for all samples. Polystyrene dissolved into the toluene solutions was used as the binding agent for each of the samples. The differences in the measured WCA values were attributed to variations in the topography and structure of these coatings.

Super-hydrophobic properties can be obtained by creating rough surfaces through assembly processes or other methods of preparing hierarchical structures *(43)*. In our study, both types of hierarchical coatings prepared from the assemblies of silica particles, either with or without polystyrene nanofibers, exhibited higher WCA values than the surfaces that were comprised of only a single type of silica particle (i.e. either large or small diameter particles). The coatings containing only the smaller silica particles and the polystyrene binder had a larger relative surface-area-to-volume ratio and, therefore, more potential points of contact with the water droplets. These surfaces exhibited the smallest WCAs of all the samples. Substrates coated with only the larger silica particles and polystyrene binder had a surface topology that hindered water infiltration and trapped pockets of air within their structures, resulting in progressively larger WCAs. All coatings containing the larger silica particles and polystyrene binder

exhibited hydrophobic WCA values (> 90°). However, the WCA values of these samples cannot be accurately determined due to the significant increase in roughness of these coatings (Figure 2). The WCA values for all of the samples containing larger silica particles were potentially underestimated and required further investigation.

To better understand the homogeneity and quality of our coatings, further WCA measurements were performed by increasing the volume of water within the applied droplets. These measurements were performed using the same conditions as mentioned above, but the water droplet volumes were increased in 10 μL increments from 10 to 100 μL. Coatings containing a single type of silica particles (e.g., only larger or smaller diameter particles) exhibited relatively consistent WCA values with increasing droplet volume (Figure 3). Due to the relatively uniform roughness and topology of these coatings, their water management properties were also fairly consistent across all applied volumes of water. Surface coatings that contained hierarchical structures prepared from progressively smaller silica particles exhibited a more significant variation in their measured WCA values at smaller droplet volumes. The WCA values for these samples did, however, reach a more consistent value when the volume of the water droplet was increased above 40 μL (i.e. critical volume for WCA stabilization on these surfaces). The average lateral separation of the tallest features in these hierarchical coatings was ~0.5 mm (Figure S1). The larger variations in WCA values (~20 to 25%) were observed for water droplet volumes below 40 μL, which could be attributed to a significant influence of the lateral variation in features on the contact area of the smaller water droplets. The hierarchical assemblies of silica particles that contained polystyrene nanofibers exhibited an average separation of ~1 mm between some its tallest features (Figure S1). The WCA values of this sample increased as the droplet volume increased above 60 μL. Variation in the WCA values also significantly decreased for droplets above 60 μL as the dimensions of the droplets were sufficiently larger than the average separation of the tallest features within these assembled coatings. A larger portion of the water droplet was, therefore, in contact with the polystyrene nanofibers at these larger droplet volumes, which trapped a more consistent volume of air within the porous network of the

assemblies and exhibited more consistent WCA values. We also observed that the water droplets adhered more strongly to the hierarchical structures at smaller water droplet volumes. These volume dependent WCA properties of the assembled coatings were, however, not observed when inverting the substrates (Figure S2). The surfaces prepared from hierarchical assemblies of silica (both with and without the polymer nanofibers) retained around 40 μL before the droplet released from its surfaces. This difference in behavior observed with increasing droplet volume for the inverted sample can be attributed to a relatively consistent contact area between the droplet and the structured surfaces. The water droplet reaches a critical volume before gravity pulls the droplet away from the inverted surfaces. Further insight into the interactions between the water droplets and the hierarchically assembled coatings was sought through pseudo dynamic WCA measurements.

Pseudo Dynamic WCA Measurements

Each of the hierarchical samples prepared by spray coating demonstrated similar properties to a rose petal. These coatings were able to pin water droplets to their surfaces and demonstrated a strong adhesion to water, yet at the same time, the water droplets were able to roll freely on the surfaces of these coatings. The water droplets adhered strongly to the structured coatings even when the substrates were oriented in either a vertical or inverted orientation (Figures S2 and S3). These WCA experiments demonstrated an inversely proportional relationship between the adhesion of the water and increases in the volume of applied water applied to the surfaces.

Previous investigations have tried to quantify the hysteresis between the advancing and receding WCAs for rose petal and rose petal-like surfaces. However, the strong adhesion of the water droplets to the structured surfaces resulted in a deformation of the receding water droplets with apparent WCA values of ~90° *(12, 13, 42)*. To better assess the adhesion of the water droplets and the hysteresis in the WCAs for our samples prepared by spray coating, we performed the WCA measurements on substrates held at a consistent 45° tilt relative to the horizontal axis. The advancing and receding WCA values were

simultaneously measured for these samples from a series of images that depicted the side profile of these surfaces (Figure S4). The WCA hysteresis measured for the samples prepared from either the smaller or larger silica particles were 30 and 25, respectively, when measured for a 10 μL water droplet at an angle of 45° (Figure 4). In contrast, the hierarchical assemblies of silica particles both with and without the inclusion of polystyrene nanofibers exhibited a hysteresis of 40 degrees (Figure 4). To further investigate surface adhesion of water, the volume of the applied water droplets were further increased to determine the critical volume that was required before the surface becomes more hydrophobic (with a reduced fraction in contact with the surfaces) such that the water droplet becomes mobile and rolls freely off the substrate. Each experiment started with a pinned water droplet (i.e. a state of high water adhesion), the volume was then increased in 10 μL increments. This process ends when the droplets roll freely off the coated substrate (i.e. a state of low water adhesion), ultimately traveling a distance of ~2 cm. The receding WCAs progressively decreased to a critical angle of ~40° for all samples with increasing water volume; this critical angle was consistently observed for all samples as the minimum WCA before the water droplet would roll off each of the coated surfaces. Those surfaces coated with only the smaller or larger silica particles reached this critical water droplet volumes of 60 and 40 μL, respectively, before becoming freely mobile. These samples did, however, maintain advancing WCAs of ~100° throughout the course of these studies (i.e. for the duration of all WCA measurements with a progressively increasing droplet volume prior to the point of roll off). The hierarchical assemblies of silica particles with and without the incorporation of polystyrene fibers exhibited roll off at water droplet volumes of 30 and 80 μL, respectively. Without the incorporation of the nanofibers, the hierarchical structure was able to pin at least 30% more water (by volume) onto its surfaces when compared to the control samples. With the inclusion of nanofibers, the surface becomes more hydrophobic, requiring 25% less water (by volume) than the control samples before the droplet becomes mobile on the surface. Both of these hierarchical structured surfaces maintained advancing WCAs of ~120° over the course of these experiments, retaining rose petal-like properties until reaching a critical volume.

The hierarchical structure of silica particles without the polymer nanofibers demonstrated a stronger adhesion to the water droplets in comparison to any of the other samples, including those prepared from either the smaller or larger silica particles alone. This increased adhesion of water for these hierarchical coatings makes these structures an excellent candidate for surfaces to be used in applications that require a well-maintained humidity, such as within air plane cabins and greenhouses *(46, 47)*. In contrast, the hierarchical structures that incorporated the polystyrene nanofibers, where water droplet mobility was observed to be proportional to the increased volume of the water droplets, could be used to efficiently capture water through a process of condensation and roll-off. Potential applications for these materials could include capturing water from fog or other humid conditions, converting the condensed water into a source of water *(48, 49)*.

Water Retention Measurements

To further demonstrate a potential application of these coatings with their tunable wetting properties, a water retention experiment was performed to assess their abilities to condense water vapor. The coated samples were placed inside an enclosed chamber along with a dish of boiling water. The samples were removed from the chamber and weighed at 15, 30, or 60 min intervals. After the completion of a 60 min interval, the samples were removed from the chamber, air dried for >1 h, and placed back into the chamber after changing their location and rotating the orientation of the substrates. Each experiment was performed at least 3 times for statistical consistency. The resulting weight of the water gained by each sample was normalized against the water retained by a planar film of polystyrene (Figure 5).

The structured films exhibited a distinct trend in their ability to condense and retain water. At a relatively short exposure to water vapor, all of the structured coatings retained more water than the planar polymer standard. The hierarchical structure with incorporated polymer nanofibers retaining 4 times as much water as the planar polystyrene film. This characteristic may be due to the surface area enhancement of the coatings containing micro- and nanostructures. However, as the duration of exposure to water vapor increased, the planar films began to exhibit a greater ability to retain surface water in

contrast to the structured coatings that exhibited an increased ability to remove water droplets from their surfaces over time (Figure 5). This observation is consistent with the pseudo dynamic WCA experiments, in which the structured coatings gradually became increasingly hydrophobic with an increase in the applied volumes of water. Optical images of each sample obtained after 60 min of exposure to the water vapor depict the formation of large water droplets on the structured coatings (Figure S5). For comparison, a piece of Teflon® film was also exposed to water vapor under the same conditions, but there was no measurable amount of water retention on this substrate during any stage of the experiment. The structured films relatively quickly condensed water vapor and maintained a consistent level of moisture on their surfaces throughout the experiments. To further demonstrate the differences in water retention characteristics of the samples prepared in these studies, each coating was mounted in a vertical orientation and exposed to a steady stream of water droplets (~2 mL in total volume) generated by a spray coater. The samples were removed from the stream of droplets and imaged against a flat surface with direct lighting to assist in the visualization of retained water droplets (Figure S6). These lighting conditions assist in observing the presence of water on these surfaces (i.e. the reflective surfaces of the droplets are easily discernable). These results further demonstrated that water droplets collected primarily on the planar polystyrene surfaces, while the hierarchical structures with incorporated polymer fibers exhibited the least amount of water retention. A limitation of these experiments is that the water collected from each of the surface structures (e.g., droplets removed from their surfaces) was not easily quantifiable. Further investigations and alternative experimental conditions are warranted to quantify the actual water collection efficiency of each coating.

The surface coatings and their methods of preparation that were demonstrated in this study rely on off-the-shelf products that are relatively inexpensive and readily available. By utilizing common materials, this process was able to achieve a reduction in cost of at least 85% (~35 USD per m^2), in comparison to other comparable surface treatments with improved water management properties, such as dispersible poly-siloxane and Teflon® particles (~209 USD per m^2). Further reductions in cost could be

realized for materials purchased at larger scales as necessary for the amounts required for coating larger surfaces.

CONCLUSIONS

Hydrophobic surfaces that simultaneously exhibited a high adhesion to water were prepared by spray coating a polystyrene binder with silica particles to create a hierarchical structure with respect to varying particle size. Different polymer structures, such as polystyrene nanofibers, were achieved by adjusting the solvent flow rates during the spray coating process. Hydrophobic WCAs were achieved with the formation of hierarchical structures either with or without the incorporation of the polymer nanofibers. However, these coating exhibit super-hydrophobic behavior in which the water droplets could roll freely on the hierarchically structured surface. The discrepancy between the measurements and observations is attributed to difficulties of accurately measuring the WCA of these rough surfaces and, thus, the reported WCA values are likely an underestimate of the actual values. Significant variations were observed in the WCA for small water droplets (diameters <5 mm) due to surface irregularities (or roughness) on length scales proportional to the dimensions of these droplets (e.g., 100's of μm). However, despite these variations, the WCAs of these hierarchical structures were more hydrophobic than any of the other coatings, such as those prepared from polystyrene binder and silica particles of a single size. The hierarchical structures assembled from silica particles of different sizes exhibited an increased adhesion towards water, pinning at least 30% more water by volume onto its surfaces when compared the control samples. The incorporation of polystyrene nanofibers into the hierarchical structure increased the mobility of water on the coated surfaces, as well as its ability to efficiently condense water vapor. This structure repelled water droplets more efficiently (i.e. requiring a 25% smaller volume of water to induce mobility of droplets) than the control samples. Further tuning of these water management properties could be investigated through the use of a monodispersed sample of silica particles to achieve a finer control over the wetting properties of the hierarchical structures. Through the preparation of different hierarchical surface coatings achieved by spray coating, a number of applications could be enabled at a relatively low

cost and over a large scale for efficiently collecting, maintaining, or otherwise managing surface bound water.

ACKNOWLEDGEMENTS

This work was supported through financial contributions from the Natural Sciences and Engineering Research Council (NSERC) of Canada and the Canada Research Chairs Program (B.D. Gates). This work made use of 4D LABS (www.4dlabs.ca) shared facilities supported by the Canada Foundation for Innovation (CFI), British Columbia Knowledge Development Fund (BCKDF), Western Economic Diversification Canada, and Simon Fraser University.

REFERENCES

1. L. Zhang, Y. Zhang, Y. Zhu, N. Wang, F. Xia, L. Jiang, Petal effect: a superhydrophobic state with high adhesive force, Langmuir 24 (2008) 4114-4149.
2. K. Cho, L.J. Chen, Fabrication of sticky and slippery superhydrophobic surfaces via spin-coating silica nanoparticles onto flat/patterned substrates, Nanotechnology 22 (2011) 445706-445720.
3. Z.H. Yang, F.C. Chen, C.W. Kuo, D.Y. Chueh, P. Chen, Hybrid contact and interfacial adhesion on well-defined periodic hierarchical pillars, Nanoscale, 5 (2013) 1018-1025.
4. K. Uchida, N. Nishikawa, N. Izumi, S. Yamazoe, H.Y.K. Mayama, S. Yokojima, S. Nakamura, K. Tsujii, M. Irie, Phototunable Diarylethene Microcrystalline Surfaces: Lotus and Petal Effects upon Wetting, Angew.Chem. Int. Ed. 49 (2010) 5942-5944.
5. Z. Cheng, M. Du, H. Lai, N. Zhang, K. Sun, From petal effect to lotus effect: a facile solution immersion process for the fabrication of super-hydrophobic surfaces with controlled adhesion, Nanoscale, 5 (2013) 2776-2783.
6. J.S. Sun, J.G. Wang, Fabrication of superhydrophobic surfaces on FRP composites: from rose petal effect to lotus effect, J. Coat. Technol. Res. 353 (2015) 1137-1142.
7. W.S.Y. Wong, G.Y. Liu, N. Rumsey-Hill, V.S.J. Craig, D.R. Nisbet, A. Tricoli, Flexible transparent hierarchical nanomesh for rose petal-like droplet manipulation and lossless transfer, Appl. Mater. Interfaces 2 (2015) 1500071.
8. J.Y. Long, P.X. Fan, D.W. Gong, D.F. Juang, H.J. Zhang, L. Li, M.L. Zhong, Superhydrophobic surfaces fabricated by femtosecond laser with tunable water adhesion: from lotus leaf to rose petal, ACS Appl. Mater. Interfaces 7 (2015) 9858-9865.
9. J. Liu, X. Lu, Z. Xin, C.L. Zhou, Preparation and surface properties of transparent UV-resistant "petal effect" superhydrophobic surface based on polybenzoxazine, Appl. Surf. Sci. 353 (2015) 1137-1141.

10. J.M. Wang, Q.L. Yang, M.C. Wang, C. Wang, L. Jiang, Rose petals with a novel and steady air bubble pinning effect in aqueous media, Soft Matter 8 (2012) 2261-2266.
11. B. Balu, V. Breedveld, D.W. Hess, Fabrication of "roll-off" and "sticky" superhydrophobic cellulose surfaces via plasma processing, Langmuir 24 (2008) 4785-4790.
12. K.Y. Yeh, K.H. Cho, A. Promraksa, C.H. Huang, C.C. Hsu, L.J. Cheng, Observation of the rose petal effect over single- and dual-scale roughness surfaces, Nanotechnology 25 (2014) 345303-245313.
13. B. Bhushan, M.P. Nosonovsky, The rose petal effect and the modes of superhydrophobicity, Trans. R. Soc. A 368 (2010) 4713-4728.
14. A.B.D. Cassie, S. Baxter, Wettability of porous surfaces, Trans. Faraday Soc. 40 (1944) 546-551.
15. R.N. Wenzel, Resistance of solid surfaces to wetting by water, Ind. Eng. Chem. 25 (1936) 998-1003.
16. X.Y. Ling, I.Y. Phang, G.J. Vancso,J. Huskens, D.N. Reinhoudt, Stable and transparent superhydrophobic nanoparticle films, Langmuir 25 (2009) 3260-3263.
17. A.C. Balazs, O. Kuksenok, A. Alexeev, Modeling the interactions between membranes and inclusions: designing self-cleaning films and resealing pores, Macromol. Theor. Simul. 18 (2009) 11-24.
18. A.K. Sasmal, C. Mondal, A.K. Sinha, S.S. Gauri, J. Pal, T. Aditya, M. Ganguly, S. Dey, Fabrication of superhydrophobic copper surface on various substrates for roll-off, self-cleaning, and water/oil separation, ACS Appl. Mater. Inter. 6 (2014) 22034-22043.
19. K. Matsukawa, Y. Matsuura, Y. Michiwaki, M. Chikaraishi, H.J. Naito, Low refractive index of polysilane-silica nanoparticle hybrids and their application for anti-reflection films, Photopolym. Sci. Technol. 22 (2009) 307-309.
20. X.L. Chen, X.H. Geng, J.M. Xue, L.N. Li, Two-step growth of ZnO films with high conductivity and high roughness, Inorg. Mater. 299 (2007) 77-81.
21. X.L. Wang, Q.F. Di, R.L. Zhang, C.Y. Gu, W.P. Ding, W. Gong, Dual drag reduction mechanism of water-based dispersion with hydrophobic nanoparticles in core microchannel and experimental verification, Acta Phys. Sin. 61 (2012) 146801-146807.
22. L. Feng, Z. Yang, J. Zhai, Y. Song, B. Liu, Y. Ma, Z. Yang, L. Jiang, D. Zhu, Superhydrophobicity of nanostructured carbon films in a wide range of pH values, Angew. Chem. Int. 42 (2003) 4217-4220.
23. J. Genzer, K. Efimenko, Creating long-lived superhydrophobic polymer surfaces, Science 290 (2000) 2130-2133.
24. L.Y. Gao, M.J. Zheng, M. Zhong, M. Li, L. Ma, Preparation and photoinduced wettability conversion of superhydrophobic β-Ga_2O_3 nanowire film, Appl. Phys. Lett. 91 (2007) 013101-013104.
25. J. Bravo, L. Zhai, Z. Wu, R.E. Cohen, M.F. Rubner, Transparent superhydrophobic films based on silica nanoparticles, Langmuir 23 (2007) 7293-7298.
26. X. Qian, Z. Zhang, L. Song, H. Liu, A novel approach to raspberry-like particles for superhydrophobic materials, J. Mater. Chem. 9 (2009) 1297-1304.
27. X. Gao, L. Jiang, Biophysics: water-repellent legs of water striders, Nature 432 (2004) 36-36.
28. Y.Y. Liu, X.Q. Chen, J.H. Xin, Hydrophobic duck feathers and their simulation on textile substrates for water repellent treatment, Bioinspir. Biomim. 3 (2008) 046007-046015.

29. G.N. Kostina, V.E. Sokolov, E.V. Romanenko, O.F. Chernova, T.N. Sidorova, V.A. Tarchevskaya, O.F. Chernova, Hydrophobic capacity of feather elements in penguins, Zool. Zh. 75 (1996) 237-248.
30. K. Autumn, M. Sitti, Y.C.A. Liang, Evidence for van der Waals adhesion in gecko setae, Proceeding of the National Academy of Sciences of the United States of America, 99 (2002) 12252-12256.
31. K. Autumn, Y.A. Liang, S.T. Hsieh, W. Zesch, W.P. Chan, T.W. Kenny, R. Fearing, R.J. Full, Adhesive force of a single gecko foot-hair, Nature, 405 (2000) 681-685.
32. M.J. Moon, J.G. Park, Fine structural analysis on the dry adhesion system of the jumping spider Plexippus setipes, Anim. Cells. Syst. 13 (2009) 161-167.
33. V. Zorba, E. Stratakis, M. Barberoglou, E. Spanakis, P. Tzanetakis, S.H. Anastasiadis, C. Fotakis, Biomimetic Artificial Surfaces Quantitatively Reproduce the Water Repellency of a Lotus Leaf, Adv. Mater. 20 (2008) 4049-4054.
34. K. Koch, B. Bhushan, Y.C. Jung, Barthlott, W. Fabrication of artificial lotus leaves and significance of hierarchical structure for superhydrophobicity and low adhesion, Soft Matter 5 (2009) 1386-1393.
35. Y.M. Zheng, X.F Gao, L. Jiang, Directional adhesion of superhydrophobic butterfly wings, Soft Matter 3 (2007) 178-182.
36. L. Feng, Y.A. Zhang, J.M. Xi, Y. Zhu, N. Wang, F. Xia, L. Jiang, Petal effect: a superhydrophobic state with high adhesive force, Langmuir 24 (2008) 4114-4119.
37. S. Choo, H.J. Choi, H. Lee, Replication of rose-petal surface structure using UV-nanoimprint lithography, Mater. Lett. 121 (2014) 170-173.
38. J.K. Chen, J.H. Wang, S.K. Fan, J.Y. Chang, Reversible hydrophobic/hydrophilic adhesive of PS-b-PNIPAAm copolymer brush nanopillar arrays for mimicking the climbing aptitude of geckos, J. Phy. Chem. C, 116 (2012) 6980-6992.
39. Y.C. Tsai, W.P. Shih, Artificial petal effect on nanofibrillar Parylene™ surface, J. Adhesion, 88 (2012) 32-54.
40. M.H. Jin, X.J. Feng, J.M. Xi, J. Zhai, K.W. Cho,L. Feng, L. Jiang, Super-hydrophobic PDMS surface with ultra-low adhesive force, Macromol. Rapid Commun. 26 (2005) 1805-1809.
41. J. Feng, B.Y. Huang, M.Q. Zhong, Fabrication of superhydrophobic and heat-insulating antimony doped tin oxide/polyurethane films by cast replica micromolding, J. Colloid Interface Sci. 336 (2009) 268-272.
42. M.T.Z. Myint, G.L. Hornyak, J. Dutta, One pot synthesis of opposing 'rose petal' and 'lotus leaf' superhydrophobic materials with zinc oxide nanorods, J. Colloid. Interface Sci. 415 (2014) 32-38.
43. J.F. Zheng, A.H. He, J.X. Li, J.A. Xu, C.C. Han, Studies on the controlled morphology and wettability of polystyrene surfaces by electrospinning or electrospraying, Polymer, 47 (2006) 7095-7102.
44. D.H. Reneker, I. Chun, Nanometre diameter fibers of polymer, produced by electrospinning, Nanotechnology, 7 (1996) 216-223.
45. S. Hoshian, V. Jokinen, V. Somerkivi, A.R. Lokanathan, S. Franssila, Robust superhydrophobic silicon without a low surface-energy hydrophobic coating, ACS Appl. Mater. Inter.7 (2015) 941-949.

46. S.T. Bement, A.R. Nassar, K. Mehta, The feasibility of rice bags as a low-cost and locally available alternative to greenhouse glazing, Proceedings of the third 2013 IEEE Global Humanitarian Technology Conference, (2013) 254-259.
47. D. Norback, T. Lindgren, G. Wieslander, Changes in ocular and nasal signs and symptoms among air crew in relation to air humidification on intercontinental flights, Scand. J. Work. Env. Hea. 32 (2006) 138-144.
48. J.K. Domen, W.T. Stringfellow, M.K. Camarillo, Fog water as an alternative and sustainable water resource, Clean Technol. Envir. 16 (2014) 235-249.
49. M. Fessehaye, S.A. Abdul-Wahab, M.J. Savage, Fog-water collection for community use, Renew Sust. Eenerg. Rev. 29 (2014) 52-62.

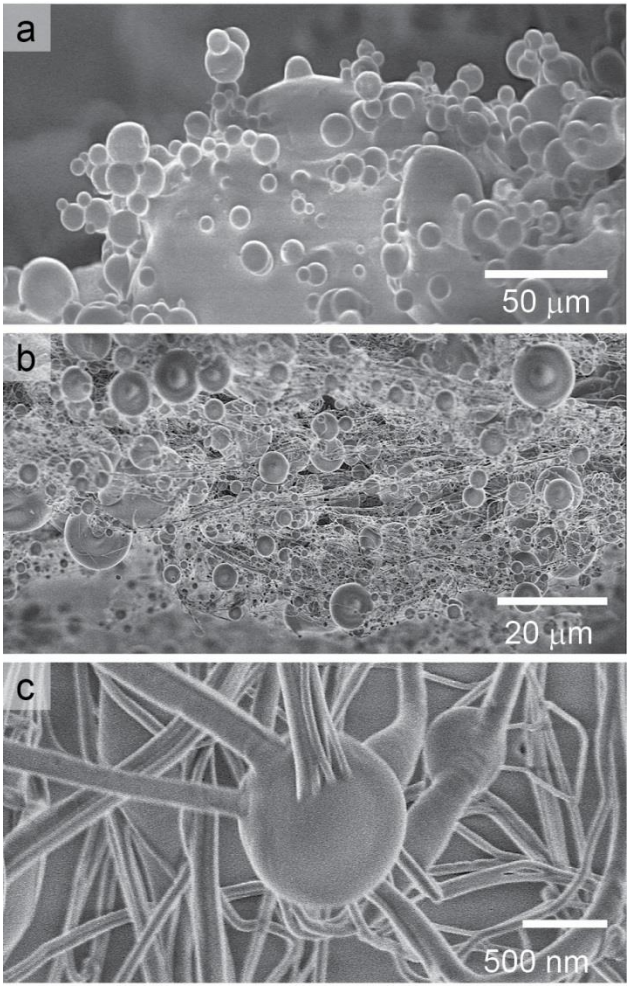

Figure 1. Scanning electron microscopy (SEM) images of structured coatings prepared by spray coating to achieve (a) hierarchically assembled silica particles, or (b) hierarchical structures of silica particles that also incorporated polystyrene nanofibers. (c) High magnification SEM image of the polystyrene nanofibers attached to smaller silica particles.

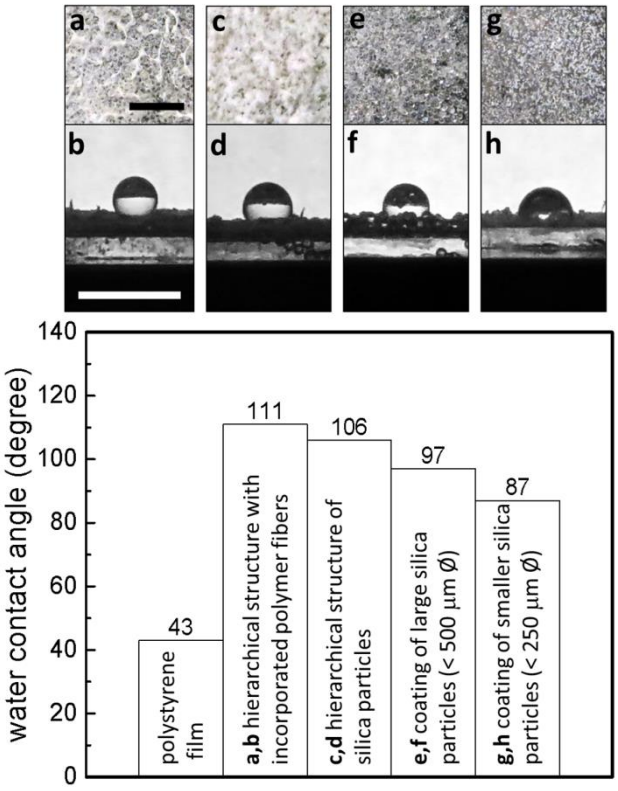

Figure 2. Static water contact angle (WCA) measurements and optical images obtained for different surface coatings prepared by spray coating mixtures of silica particles and polystyrene binder. Optical images (viewed from the top down and as a side-profile, respectively) correspond to coatings prepared from: (a, b) hierarchical assemblies of silica particles that incorporate polymer nanofibers; (c, d) hierarchical assemblies of silica particles; (e, f) only the larger silica particles; and (g, h) only the smaller silica particles. All scale bars are 5 mm. The corresponding average WCAs for these coatings are summarized in the bar graph along with the WCA measured for a film prepared with only polystyrene.

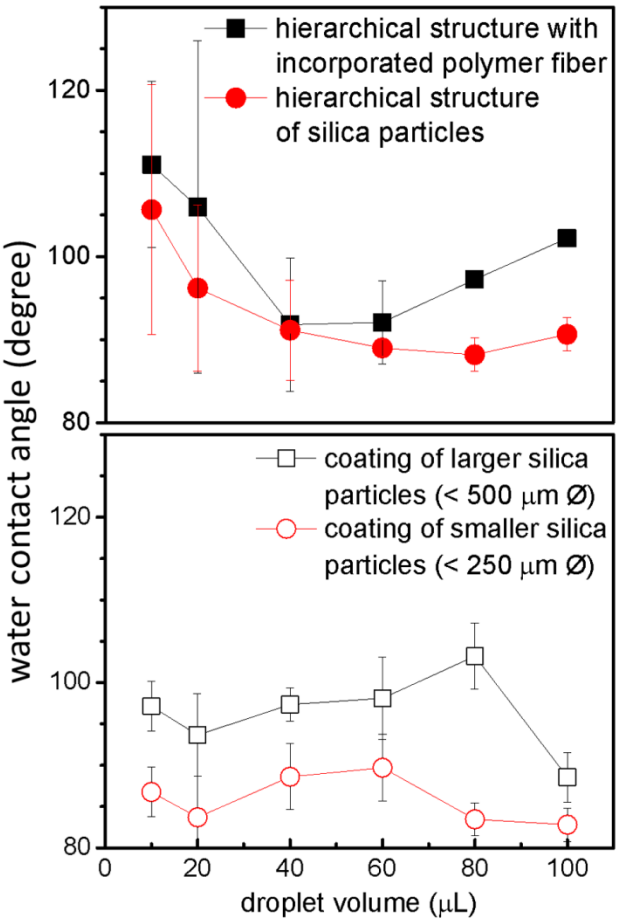

Figure 3. Static water contact angle measurements for various structured surfaces prepared by spray coating processes. Measurements are reported as a function of increasing water droplet volume. Error bars were calculated as the standard deviation of at least five measurements obtained from different locations on the same substrate.

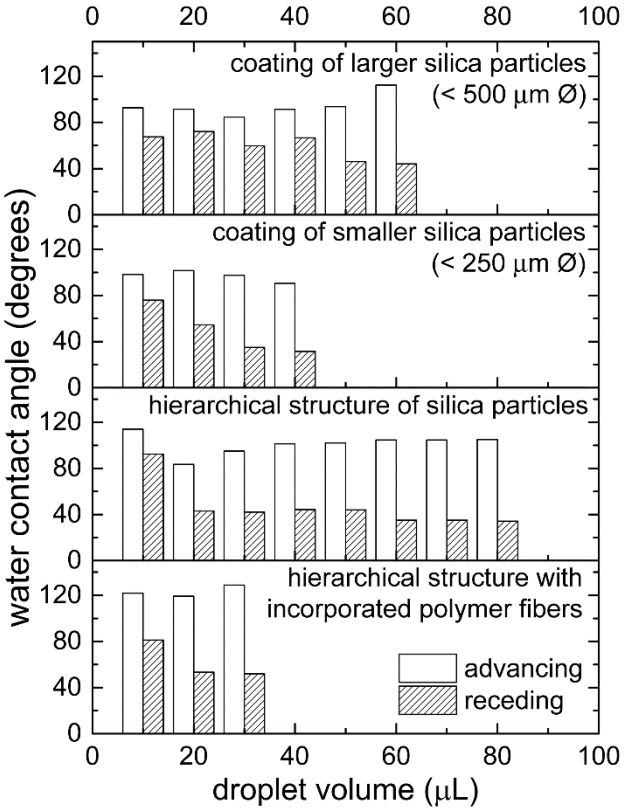

Figure 4. The advancing and receding water contact angles for structured surfaces tilted at 45 degrees. Measurements were made with respect to increases in the volume of the applied water droplet.

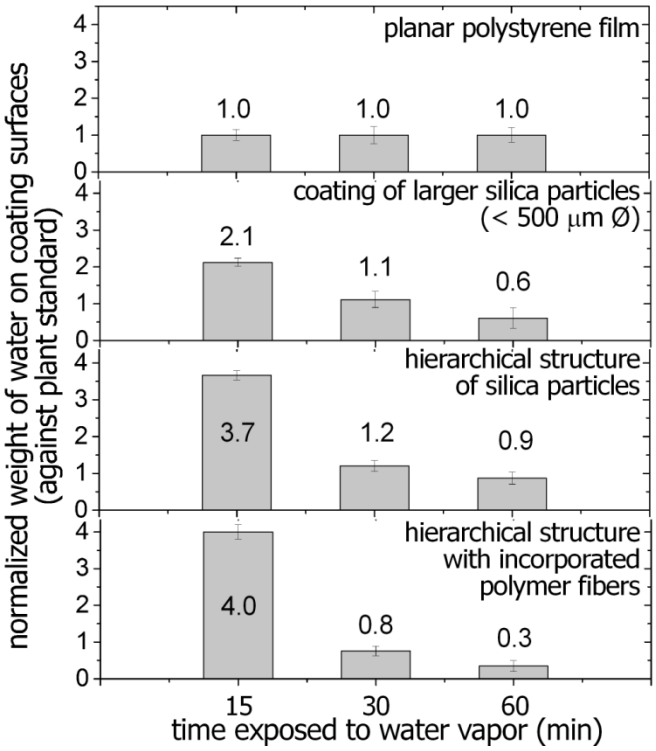

Figure 5. The normalized weight of water on the surfaces of different coatings, standardized against a planar film of polystyrene. The mass of water retained on each coating was measured after 15, 30, and 60 min of exposure to water vapor.

TABLE OF CONTENTS (TOC) ABSTRACT GRAPHIC